

AD-A073 235

AEROSPACE CORP EL SEGUNDO CA AEROPHYSICS LAB

F/G 20/9

A SIMPLE METHOD FOR DECONVOLUTING CROSS-SECTION DATA, (U)

AUG 79 M EPSTEIN

F04701-78-C-0079

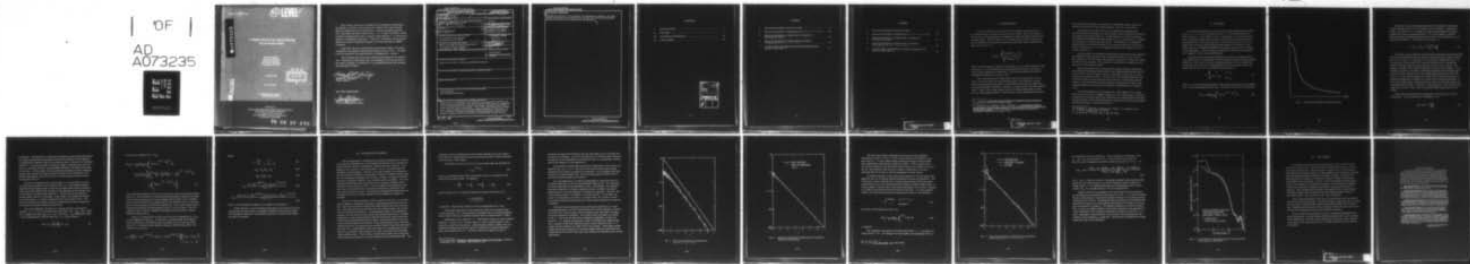
UNCLASSIFIED

TR-0079(4940-01)-6

SAMSO-TR-79-68

NL

| DF |
AD
A073235



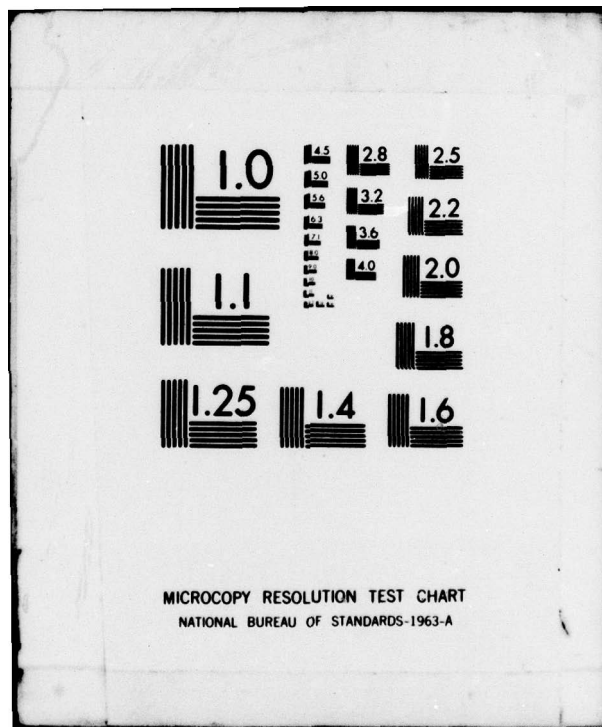
END

DATE

FILMED

10-79

DDC



■ A 073235

A Sample Notice for Prequalification
Contractor Status

Prepared for
SPACE AND MISSILE SYSTEMS ORGANIZATION
AIR FORCE SYSTEMS COMMAND
Los Angeles Air Force Station
P.O. Box 92960, Worldwide Postal Center
Los Angeles, Calif. 90009

79 08 27 072

This interim report was submitted by The Aerospace Corporation, El Segundo, CA 90245, under Contract No. F04701-78-C-0079 with the Space and Missile Systems Organization, Contracts Management Office, P.O. Box 92960, Worldway Postal Center, Los Angeles, CA 90009. It was reviewed and approved for The Aerospace Corporation by W. R. Warren, Jr., Director, Aerophysics Laboratory. Gerhard E. Aichinger was the project officer for Mission-Oriented Investigation and Experimentation (MOIE) Programs.

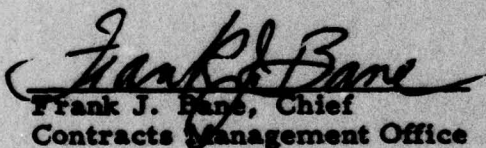
This report has been reviewed by the Information Office (OI) and is releasable to the National Technical Information Service (NTIS). At NTIS, it will be available to the general public, including foreign nations.

This technical report has been reviewed and is approved for publication. Publication of this report does not constitute Air Force approval of the report's findings or conclusions. It is published only for the exchange and stimulation of ideas.



Gerhard E. Aichinger
Project Officer

FOR THE COMMANDER



Frank J. Bane, Chief
Contracts Management Office

UNCLASSIFIED

SECURITY CLASSIFICATION OF THIS PAGE (When Data Entered)

REPORT DOCUMENTATION PAGE		READ INSTRUCTIONS BEFORE COMPLETING FORM
1. REPORT NUMBER 12 SAMSO-TR-79-68	2. GOVT ACCESSION NO.	3. RECIPIENT'S CATALOG NUMBER
4. TITLE (and Subtitle) 6 A SIMPLE METHOD FOR DECONVOLUTING CROSS-SECTION DATA	5. TYPE OF REPORT & PERIOD COVERED Interim	
7. AUTHOR(s) 10 Melvin Epstein	6. PERFORMING ORG. REPORT NUMBER TR-0079(4940-01)-6	
9. PERFORMING ORGANIZATION NAME AND ADDRESS The Aerospace Corporation El Segundo, Calif. 90245	10. PROGRAM ELEMENT, PROJECT, TASK AREA & WORK UNIT NUMBERS 12 25P	
11. CONTROLLING OFFICE NAME AND ADDRESS Space and Missile Systems Organization Air Force Systems Command Los Angeles, Calif. 90009	12. REPORT DATE 11 31 Aug 1979	
14. MONITORING AGENCY NAME & ADDRESS (if different from Controlling Office)	13. NUMBER OF PAGES 20	
	15. SECURITY CLASS. (of this report) Unclassified	
	15a. DECLASSIFICATION/DOWNGRADING SCHEDULE	
16. DISTRIBUTION STATEMENT (of this Report) Approved for public release; distribution unlimited		
17. DISTRIBUTION STATEMENT (of the abstract entered in Block 20, if different from Report)		
18. SUPPLEMENTARY NOTES		
19. KEY WORDS (Continue on reverse side if necessary and identify by block number) Cross sections Deconvolution techniques		
20. ABSTRACT (Continue on reverse side if necessary and identify by block number) When atomic or molecular cross sections are measured by electron- or molecular-beam techniques, the energy spread of the beam is responsible for the measurement to be related to an energy averaged cross section rather than the true cross section. These two cross sections are related by an integral equation involving the energy distribution of the beam. A new numerical technique is presented that facilitates the solution of the integral equation such that the effects of experimental scatter on the		

DD FORM 1473
(FACSIMILE)

UNCLASSIFIED

SECURITY CLASSIFICATION OF THIS PAGE (When Data Entered)

409 367

UNCLASSIFIED

SECURITY CLASSIFICATION OF THIS PAGE(When Data Entered)

ABSTRACT (Continued)

stability and accuracy of the solution are significantly reduced. An exact analytical solution is also derived for the case of a truncated Maxwellian energy distribution with constant beam temperature.



UNCLASSIFIED

SECURITY CLASSIFICATION OF THIS PAGE(When Data Entered)

CONTENTS

I.	INTRODUCTION	5
II.	ANALYSIS	7
III.	ILLUSTRATIVE EXAMPLE	13
IV.	CONCLUSIONS	23

ACCESSION for	
NTIS	White Section <input checked="" type="checkbox"/>
DOC	Buff Section <input type="checkbox"/>
UNANNOUNCED	<input type="checkbox"/>
JUSTIFICATION _____	
BY _____	
DISTRIBUTION/AVAILABILITY CODES	
Distr.	AVAIL. and/or SPECIAL
A	

FIGURES

1.	Characteristic Shape of Resonance Peak	8
2.	Numerical Simulation of Experiment ($S = e^{-V}$, $t = 1$, $\delta = 0.1$).	16
3.	Numerical Simulation of Experiment--Evaluation of Smoothing Procedure	17
4.	Numerical Simulation of Experiment--Calculated Cross Section ($S = e^{-U}$, $t = 1$, $\delta = 0.1$)	19
5.	F_2 Dissociative Attachment Cross Section Obtained From Chantry's Data (Ref. 1)	21

FIGURES

1.	Characteristic Shape of Resonance Peak	8
2.	Numerical Simulation of Experiment ($S = e^{-V}$, $t = 1$, $\delta = 0.1$).	16
3.	Numerical Simulation of Experiment--Evaluation of Smoothing Procedure	17
4.	Numerical Simulation of Experiment--Calculated Cross Section ($S = e^{-U}$, $t = 1$, $\delta = 0.1$)	19
5.	F ₂ Dissociative Attachment Cross Section Obtained From Chantry's Data (Ref. 1)	21

I. INTRODUCTION

A typical problem in the measurement of collision cross sections is the determination of resonance peaks of narrow width. Often, the energy resolving power of the apparatus is inadequate to define clearly the shape of the resonance peak. When an electron or molecular beam is used, the quantity that is measured is an energy-averaged cross section $\bar{\sigma}$ that is related to the true cross section σ by

$$\bar{\sigma}(V_a) = \frac{\int_0^{\infty} V\sigma(V)f(V; V_a, \tau) dV}{\int_0^{\infty} Vf(V; V_a, \tau) dV} \quad (1)$$

where V is the energy of a particle in the beam, V_a is a characteristic energy of the beam, τ is a characteristic energy spread of the beam, and $f(V; V_a, \tau)$ is the energy distribution of the beam. If the energy spread of the beam is negligible compared to V_a , $\bar{\sigma}(V_a) = \sigma(V)$.

The measurement of the distribution function f is generally very difficult. For this reason, the approximation that $\sigma = \bar{\sigma}$ sometimes is made. If the energy spread of the beam is made sufficiently small, this approximation obviously will be tolerable. However, in many cases of practical interest (Refs. 1 and 2), the energy spread cannot be reduced sufficiently to justify the use of this approximation. In these cases, even an approximate estimate

¹P. J. Chantry, Attachment Measurements in Halogen Bearing Molecules, Westinghouse R&D Center (March 1978).

²P. Mahadevan, M. Epstein, and R. Hofland, Jr., Final Report: Plasma Cross-Section Measurements Relevant to Atmospheric-Pressure High-Power DF/HF Chain Lasers, ATR-78(7585)-1, The Aerospace Corporation, El Segundo, California (31 August 1978).

of the distribution function could result in a significantly better estimate of the true cross section if the integral equation, Eq. (1), can be solved.

In principle, the solution of Eq. (1) is relatively straightforward. Several numerical techniques have been devised, most of which are variations of a collocation technique (Ref. 3). In this approach, it is assumed that experimental measurements have been made at, e.g., N values of V_a . N values of V at which σ is desired are then chosen. The function σ is interpolated analytically between adjacent values of V so that by writing Eq. (1) N times (at the N values of V_a), a set of N algebraic equations are obtained for the N unknown values of σ .

Unfortunately, the numerical computations associated with this approach are difficult to perform because the matrices that have to be inverted are ill-conditioned. The accuracy of the method is, therefore, rather poor unless the data are very smooth. This condition is not likely to be satisfied for the case of a narrow resonance peak.

Some researchers have recognized this problem and have approached the problem of smoothing the data with a very sophisticated technique (Ref. 4). In many of the cases of interest, the use of this type of technique, provides significantly improved results. However, since this sophisticated approach involves the high-frequency filtering of the data (to eliminate experimental scatter), it may still fail to produce adequate results when the width of the resonance peak is as small as a few times the uncertainty in the resolution of V_a .

A numerical approach is described here, which appears to be useful when the cross section is rapidly varying over some energy range, but slowly varying over an energy range large compared to the energy spread of the beam. An exact solution of the integral equation is also given for a form of the distribution function that is of practical interest.

³K. Berkling, R. Helbing, K. Kramer, H. Pauly, C. H. Schlier, and P. Toschek, Z. Phys., 166, 406 (1962).

⁴J. D. Morrison, J. Chem. Phys., 39, 200 (1963)

II. ANALYSIS

It is assumed that the true cross section has the qualitative form shown in Fig. 1, i.e., a narrow resonance peak at $V = 0$ and smooth behavior at large values of V . The method, in fact, is applicable to cross-section functions containing multiple peaks of arbitrary locations provided the measurements extend over an energy range that is large compared to the sum of the widths of the resonance peaks and the energy spread τ of the beam. This method has been developed specifically for two particular forms of the beam-energy distribution. These results are sufficient to indicate how the method can be applied to other energy distributions.

The particular beam-energy distribution considered is appropriate for many experimental investigations of cross sections for electron heavy-particle collisions. If the beam is formed by emitting electrons from a cathode and accelerating them through an anode aperture to form an electron beam, the distribution function can be reasonably approximated by

$$f = \begin{cases} 0 & V < V_a \\ e^{-(V - V_a)/\tau} & V \geq V_a \end{cases} \quad (2)$$

where V_a is the accelerating potential of the anode with respect to the cathode, and τ is the energy spread of the beam. For this form of f , Eq. (1) becomes

$$\bar{\sigma}(V_a) = \frac{1}{\tau(\tau + V_a)} \int_{V_a}^{\infty} V \sigma(V) e^{-(V - V_a)/\tau} dV \quad (3)$$

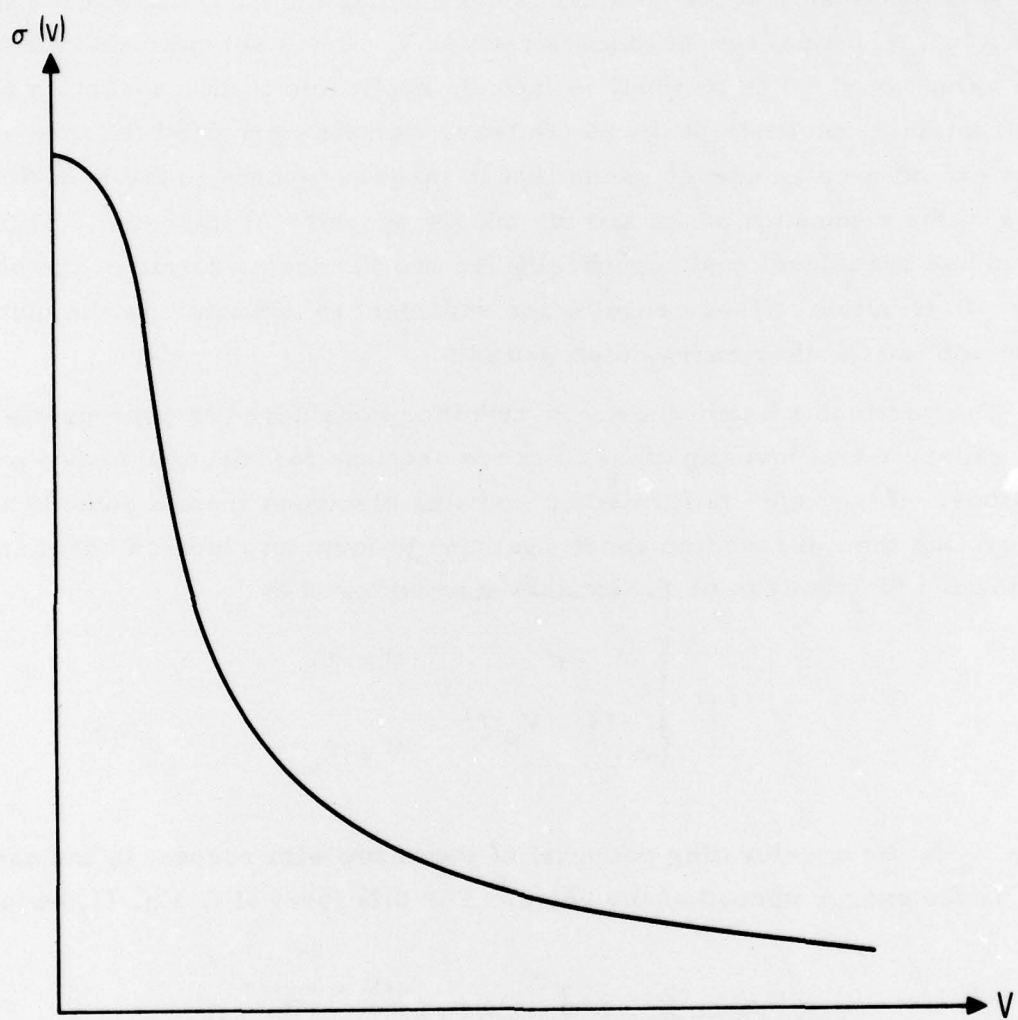


Fig. 1. Characteristic Shape of Resonance Peak

Before the numerical technique that has been developed is described, an exact solution of Eq. (3) for the special case of constant τ is discussed briefly. The quantity τ is a constant when the energy spread of the beam is independent of the accelerating potential. The exact solution is obtained almost trivially by differentiating both sides of Eq. (3) with respect to V_a and solving the result for σ . The solution for constant τ is

$$\sigma(V_a) = \bar{\sigma}(V_a) - \frac{\tau(\tau + V_a)}{V_a} \frac{d\bar{\sigma}}{dV_a} \quad (4)$$

In practice, this method has certain distinct advantages and disadvantages. The primary advantage is that no elaborate computations are needed to calculate σ (if, of course, τ is assumed to be constant and adequately known). On the other hand, the derivative of $\bar{\sigma}$ must be calculated, and, consequently, scatter in the data could seriously affect the accuracy of the results. The problem of scatter can be reduced somewhat by one of two techniques. In one technique, the data is smoothed. Relatively unsophisticated smoothing algorithms should be adequate to provide a substantial improvement in the estimate of σ . In the other technique, the scatter often becomes large when the experimental apparatus is pushed to the limits of its resolving capability. A beam with a larger energy spread tends to be easier to deal with and has correspondingly less scatter. Therefore, if the parameter τ can be defined with sufficient accuracy, a beam with an extremely small energy spread is not needed.

Note that near the peak of the measured cross section, Eq. (4) is indeterminate. By the application of L'Hospital's rule,

$$\sigma(0) = \bar{\sigma}(0) - \tau^2 \frac{d^2 \bar{\sigma}}{dV_a^2} \quad (5)$$

is obtained. The difficulty of computing acceptably accurate second derivatives from experimental data would appear to limit the usefulness of this approach in obtaining the maximum value of the resonance peak. However, for moderate values of τ , it may be possible to minimize scatter so that the curve of $\bar{\sigma}$ versus V_a is relatively smooth, and a tolerable estimate of $d^2\sigma/dV_a^2$ at the origin can be made. Various types of data smoothing techniques have been developed that provide estimates for upper and lower bounds for the derivatives of the function being fitted, which can be used to estimate upper and lower bounds for the peak value of σ .

For the more general case of nonconstant τ , it is necessary to resort to a numerical technique for the solution of Eq. (3). The present technique requires that the energy range covered by the experiment be large compared to the sum of the widths of the resonance peaks appearing in the energy interval of interest, and large with regard to τ . In this case, there will be an energy range in which $\sigma \approx \bar{\sigma}$ because, in that range, the distribution function is, to first order, a δ function compared to the cross section curve. It is most convenient if that region occurs at energies that are large compared to the energy at which the resonance peak occurs.

For such conditions, the value of σ at large energies is measured directly, i.e., $\sigma = \bar{\sigma}$ for V_a greater than same value, e.g., V_{a_0} . For a value of V_a , slightly less than V_{a_0} , e.g., V_{a_1} , and if $V_{a_0} - V_{a_1}$ sufficiently small, σ can be approximated in the interval $V_{a_1} \leq V \leq V_{a_0}$ by means of

$$\sigma(V) = \sigma_0 + \frac{\sigma_1 - \sigma_0}{V_1 - V_0} (V - V_0) \quad (6)$$

If Eq. (3) is evaluated at $V_a = V_{a_1}$,

$$\begin{aligned}\bar{\sigma}(V_{a_1}) &= \frac{1}{\tau_1(\tau_1 + V_{a_1})} \int_{V_{a_1}}^{\infty} V \sigma(V) e^{-\left(V - V_{a_1}\right)/\tau_1} dV \\ &= \frac{1}{\tau_1(\tau_1 + V_{a_1})} \left\{ \int_{V_{a_1}}^{V_{a_0}} V \left[\sigma_0 + \frac{\sigma_1 + \sigma_0}{V_1 - V_0} (V - V_0) \right] e^{-\left(V - V_{a_1}\right)/\tau_1} dV \right. \\ &\quad \left. + \int_{V_{a_0}}^{\infty} V \bar{\sigma}(V) e^{-\left(V - V_{a_1}\right)/\tau_1} dV \right\} \quad (7)\end{aligned}$$

where the approximation $\sigma = \bar{\sigma}$ for $V \geq V_{a_0}$ has been used in the second integral in Eq. (7). If the interest is centered on determining the magnitude and shape of the resonance peak(s), the second integral will be small, and a negligible error will be incurred if $\bar{\sigma}$ is approximated in any suitable way for V_a greater than the energy range covered in the experiment. If V_{a_1} is an energy at which $\bar{\sigma}$ has been measured, the only unknown in Eq. (7) is $\sigma_1 \equiv \sigma(V_{a_1})$. The first integral in Eq. (7) can be evaluated analytically, and the result is a linear algebraic equation for σ_1 .

When σ_1 is determined, the same process can be repeated at $V_a = V_{a_2}$, a value slightly less than V_{a_1} . In this way, a marching type of calculation can be constructed, which permits the calculation of σ_n at each V_{a_n} all the way to $V_a = 0$, with one linear algebraic equation solved at each step. The result for $\sigma_i \equiv \sigma(V_i)$ is,

$$\sigma_i = \frac{1}{A_{ii}} \left[(\tau_i + V_i) e^{-(V_i/\tau_i)} \bar{\sigma}_i + B_{ii} \sigma_{i-1} - \sigma_0 V_0 e^{-(V_0/\tau_i)} - k \sum_{j=1}^{i-1} (A_{ij} \sigma_j - B_{ij} \sigma_{j-1}) \right]$$

$$i = 1, 2, \dots, n \quad (8)$$

where

$$k = \begin{cases} 0 & i = 1 \\ 1 & i = 2, 3, \dots, N \end{cases} \quad (9)$$

$$A_{ij} = v_{j-1} C_{ij} - D_{ij} \quad (10)$$

$$B_{ij} = v_j C_{ij} - D_{ij} \quad (11)$$

$$C_{ij} = \frac{(\tau_i + v_j) e^{-(v_j/\tau_i)} - (\tau_i + v_{j-1}) e^{-(v_{j-1}/\tau_i)}}{v_{j-1} - v_j} \quad (12)$$

$$D_{ij} = \frac{(2\tau_i^2 + 2\tau_i v_j + v_j^2) e^{-(v_j/\tau_i)} - (2\tau_i^2 + 2\tau_i v_{j-1} + v_{j-1}^2) e^{-(v_{j-1}/\tau_i)}}{v_{j-1} - v_j} \quad (13)$$

and $N + 1$ is the number of values of V at which $\bar{\sigma}$ is measured.

At the i 'th step, σ can be calculated directly from the value of $\bar{\sigma}$ at the i 'th step and from the values of σ already calculated in the previous steps. The calculation, therefore, is extremely rapid and, as shown in the following section, accurate.

III. ILLUSTRATIVE EXAMPLE

The usual approach to validating the technique developed here would be to perform the calculation for a set of experimental data and to compare the results with the results of calculations obtained with other methods. This approach has, however, several drawbacks. First, no suitable data are available in this laboratory. Second, of the data available in the literature, the experimental conditions are generally not given in sufficient detail to permit an unambiguous comparison to be made. Further, in order to compare with other calculation methods, those methods must be available. The more sophisticated (and therefore presumably more accurate) methods involve moderate-to-long computer codes. Even if an effort to develop those codes were made, the results of the comparisons would not be conclusive since none of the methods are exact. Comparisons with published calculations are generally inconclusive because details of the smoothing are usually not available.

Because of these drawbacks, another approach was taken. It would be ideal to apply the calculation technique to experimental data to estimate the true cross section and then compare the result with the real true cross section. Since the real true cross section is never known exactly, the calculation was carried out as follows: An analytically simple, but qualitatively, realistic form for the true cross section was assumed and used in a thought experiment. It was assumed that an electron beam with a given energy distribution interacted with the gas in question, and measurements were made of the energy averaged cross section. If the measurements were made with infinite precision, the measured cross section could be obtained by quadrature from Eq. (1). A perturbation of the exact value of $\bar{\sigma}$ was generated at each value of V_a by Monte Carlo techniques in order to simulate the unavoidable experimental scatter. These values, which include scatter with a specified value of standard deviation, were then treated as raw experimental data. The

comparison of the calculated true cross section with the true cross section from which the "experimental" data were derived provides a direct evaluation of the accuracy of the method.

Accordingly, the form for the true cross section that was selected was

$$\sigma = \sigma_0 e^{-\left(\frac{V}{V_\sigma}\right)} \quad (14)$$

where σ_0 is the peak value of the cross section and V_σ is a measure of the width of the resonance peak. By defining

$$v = \frac{V}{V_\sigma} \quad S = \frac{\sigma}{\sigma_0} \quad \bar{S} = \frac{\bar{\sigma}}{\sigma_0} \quad t = \frac{T}{V_\sigma} \quad (15)$$

and by means of Eq. (1) with the distribution function given by Eq. (2),

$$\bar{S} = \frac{t + (1+t)v}{(1+t)^2(t+v)} \quad (16)$$

is obtained. Note that this result is true for the general case $t = t(v)$.

The thought experiment is then performed under the assumption that, at each value of v , the "measurement" is sampled from a normal distribution with a mean of $\bar{S}(v)$ and a standard deviation that is a fixed fraction δ of $\bar{S}(v)$.

Calculations were made for $t = 1$. Thirty three values of v were selected between $v = 0$ and $v = 10$. At each value of v , three "measurements" were made for a total of 99 data points. Approximately random numbers were obtained by selecting the last four digits in a tabulation of natural logarithms given to five places (Ref. 5). The first of those four digits was used to

⁵ R. S. Burington, Handbook of Mathematical Tables and Formulas, Handbook Publishers, Inc., Sandusky, Ohio (1953) p. 251.

determine the sign of the deviation from the mean (plus for an even digit and minus for an odd digit). Any minor deviation from a strictly random selection of numbers can be interpreted as modeling the bias in an experiment and thus adds to the analogy to a real experiment.

The results of numerically simulating an experiment in this manner are shown in Fig. 2 for $\delta = 0.1$. The true cross section and the exact energy-averaged cross section are shown for comparison. For this particular realization of the "experimental" data, all of the data points are within $\pm 20\%$ of the exact energy-averaged cross section.

In a real experiment, it would be appropriate to smooth the data if it is believed that there is no fine structure that might be lost. The smoothing interval is generally chosen with this in mind. Accordingly, the simulated data were subjected to a simple smoothing routine, by fitting, in a least-squares sense, successive groups of 15 points by parabolas. However, this crude fitting technique, constitutes a two-edged sword. On one edge, the scatter is eliminated; on the other, in regions where the scatter is small, an error is introduced because the true cross section cannot be fit exactly by a parabola.

The exact energy-averaged cross section was subjected to the same smoothing procedure, and the resultant data were used to calculate σ with the use of Eq. (8) in order to assess the sensitivity of the calculation technique to errors induced by smoothing. The results of this calculation are shown in Fig. 3. The error introduced by smoothing is negligible, except very close to $v = 0$. Careful consideration of Eqs. (8) through (13) indicates that this is because of the finite difference nature of the calculation near $v = 0$ rather than the existence of a peak in the cross section. From these results, it appears that the calculation of resonance peaks located at least 20% of the energy spread of the beam away from zero would not be affected by the smoothing process.

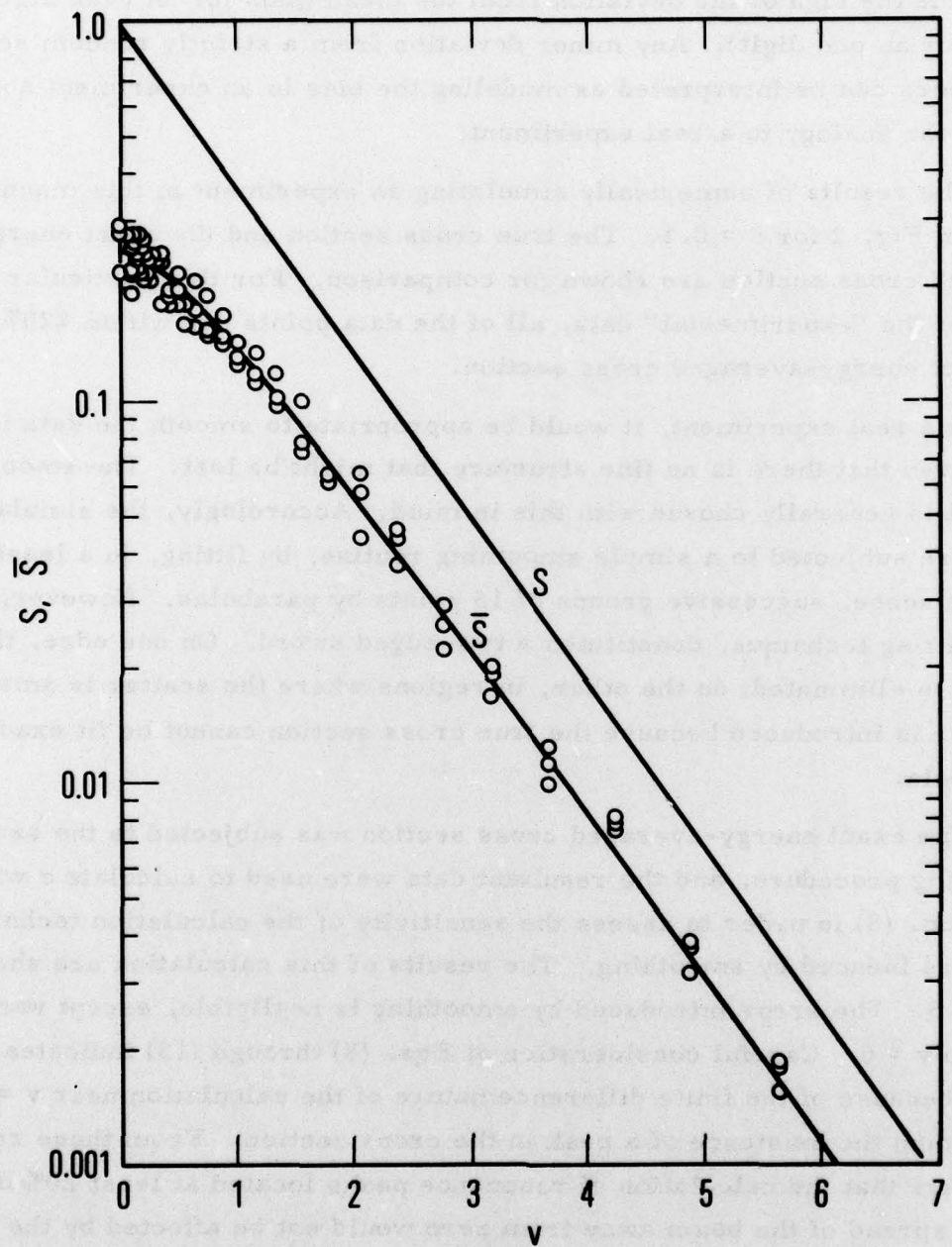


Fig. 2. Numerical Simulation of Experiment
 $(S = e^{-V}, t = 1, \delta = 0.1)$

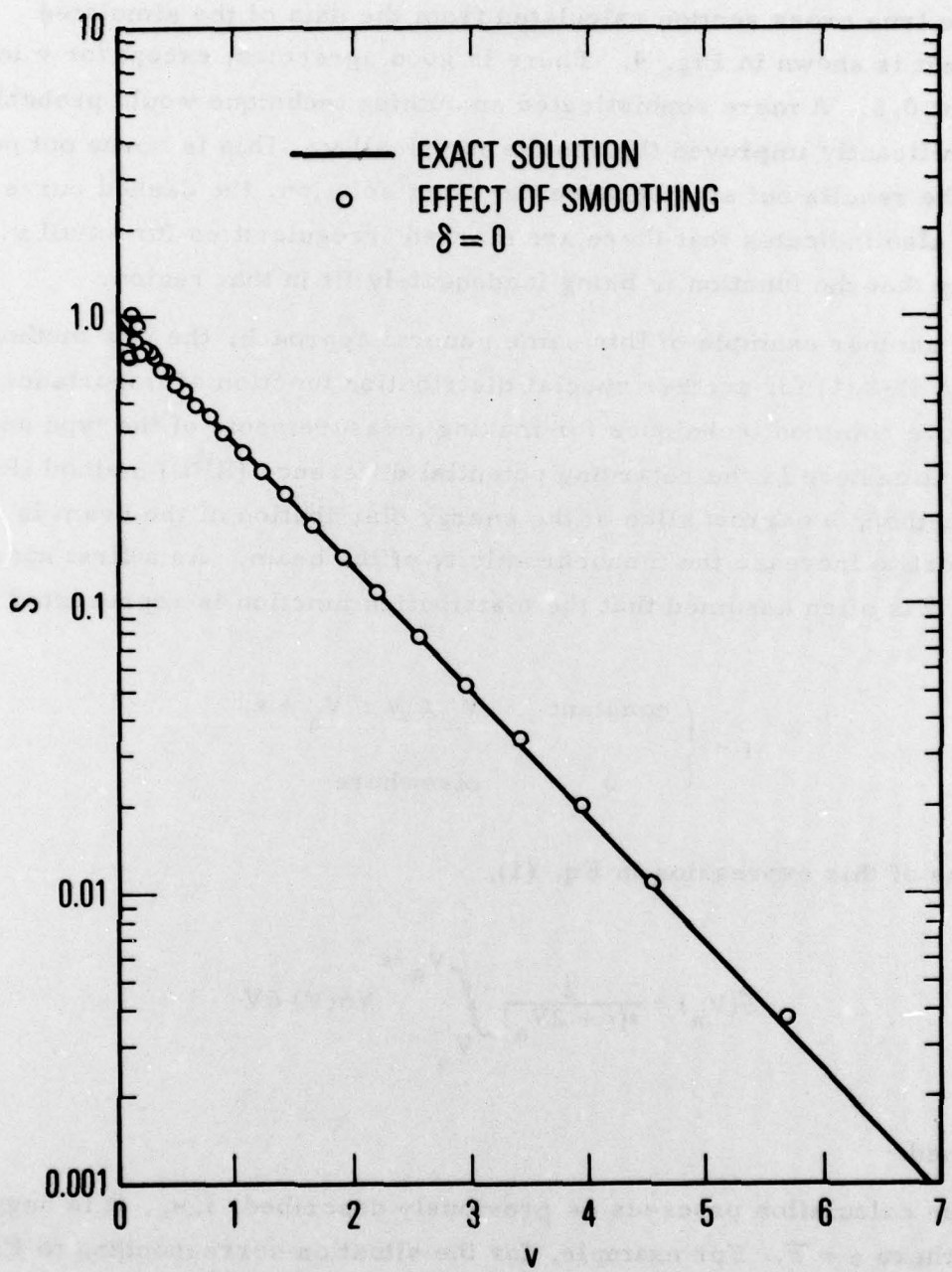


Fig. 3. Numerical Simulation of Experiment--Evaluation of Smoothing Procedure

The true cross section calculated from the data of the simulated experiment is shown in Fig. 4. There is good agreement except for v less than about 0.5. A more sophisticated smoothing technique would probably have significantly improved the results for small v . This is borne out not only by the results but also because the exact solution, the dashed curve from Eq. (4), also indicates that there are marked irregularities for small v , indicating that the function is being inadequately fit in that region.

As another example of this same general approach, the new method was applied to Eq. (1) for another special distribution function of importance. One of the more common techniques for making measurements of the type under consideration here is the retarding potential difference (RPD) method (Ref. 6). In this method, a narrow slice of the energy distribution of the beam is selected in an effort to increase the monochromicity of the beam. As a first approximation, it is often assumed that the distribution function is represented by

$$f = \begin{cases} \text{constant} & V_a \leq V \leq V_a + \epsilon \\ 0 & \text{elsewhere} \end{cases} \quad (17)$$

By means of this expression in Eq. (1),

$$\bar{\sigma}(V_a) = \frac{2}{\epsilon(\epsilon + 2V_a)} \int_{V_a}^{V_a + \epsilon} V\sigma(V) dV \quad (18)$$

is obtained.

The calculation proceeds as previously described, i. e., it is begun in a region where $\sigma \sim \bar{\sigma}$. For example, for the situation corresponding to Fig. 1,

⁶R. E. Fox, Rev. Sci. Instr. 26, 1101 (1955).

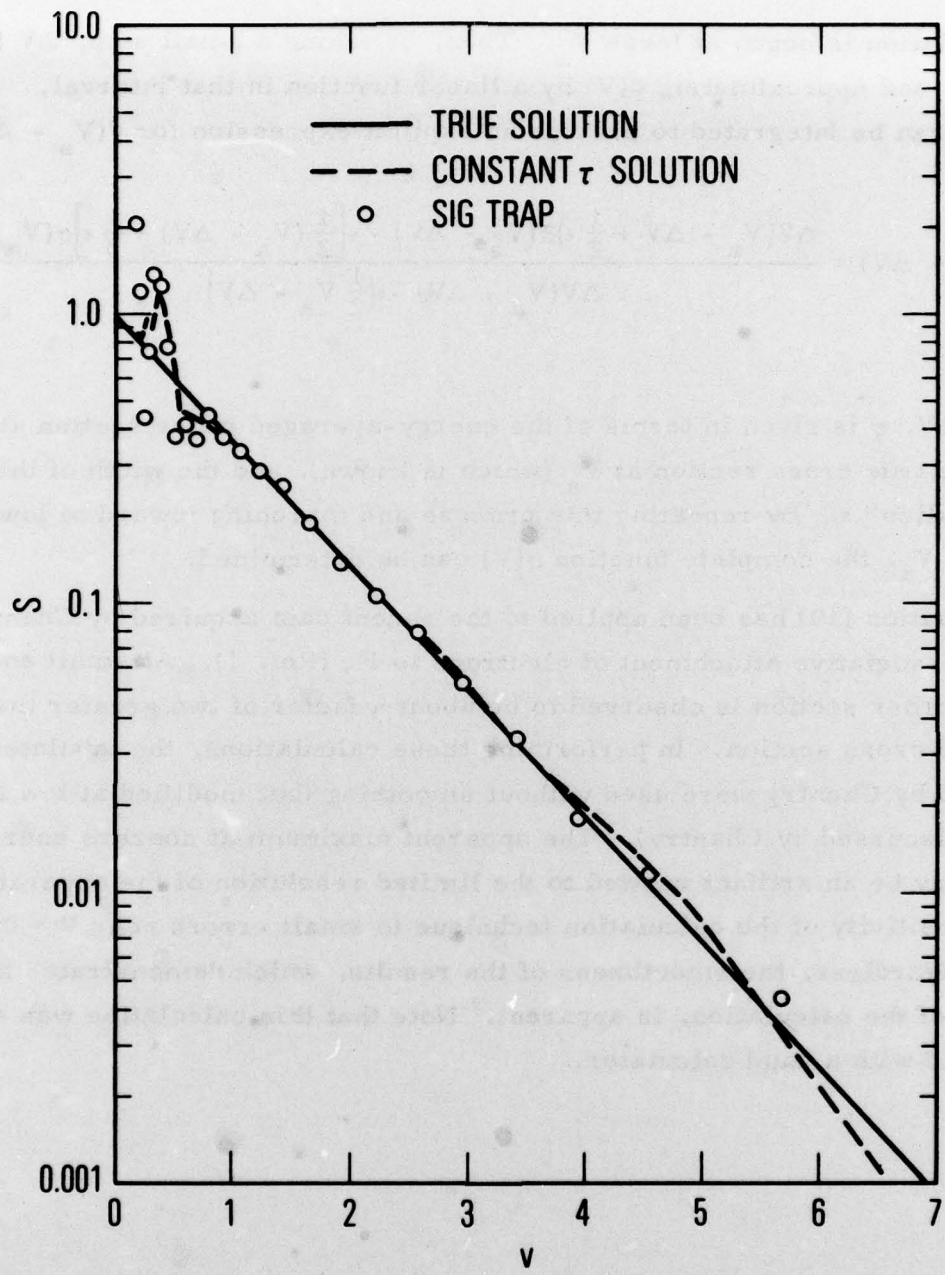


Fig. 4. Numerical Simulation of Experiment--Calculated Cross Section ($S = e^{-U}$, $t = 1$, $\delta = 0.1$)

the calculation is begun at large V_a . Then, by taking a small step, ΔV to $V_a - \Delta V$, and approximating $\sigma(V)$ by a linear function in that interval, Eq. (18) can be integrated to provide an explicit expression for $\sigma(V_a - \Delta V)$

$$\sigma(V_a - \Delta V) = \frac{\Delta V(V_a - \Delta V + \frac{1}{2}\epsilon)\bar{\sigma}(V_a - \Delta V) - \epsilon\left[\frac{1}{2}(V_a - \Delta V) + \frac{1}{3}\epsilon\right]\sigma(V_a)}{\Delta V(V_a - \Delta V) - \epsilon\left(\frac{1}{2}V_a - \Delta V\right)}$$
(19)

At $V_a - \Delta V$, σ is given in terms of the energy-averaged cross section at that point, the true cross section at V_a (which is known), and the width of the energy "slice" ϵ . By repeating this process and marching inward to lower values of V_a , the complete function $\sigma(V)$ can be determined.

Equation (19) has been applied to the recent data acquired by Chantry for the dissociative attachment of electrons to F_2 (Ref. 1). At small energies, the true cross section is observed to be about a factor of two greater than the measured cross section. In performing these calculations, the tabulated data presented by Chantry were used without smoothing (but modified at low energies as discussed by Chantry). The apparent maximum at nonzero energy in Fig. 5 may be an artifact related to the limited resolution of the apparatus or to the sensitivity of the calculation technique to small errors near $V = 0$, or both. Regardless, the smoothness of the results, which demonstrates the stability of the calculation, is apparent. Note that this calculation was easily performed with a hand calculator.

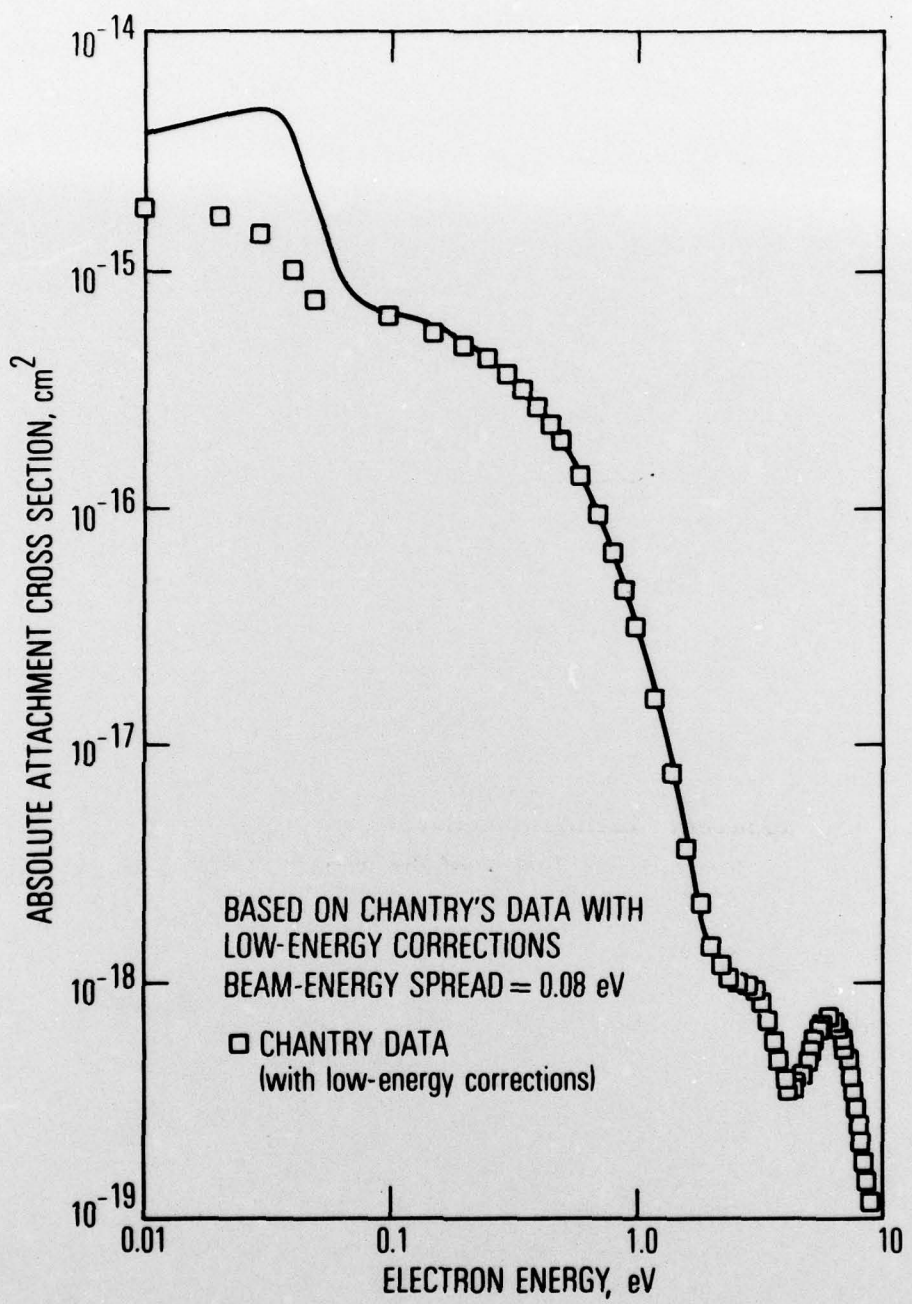


Fig. 5. F_2 Dissociative Attachment Cross Section Obtained From Chantry's Data (Ref. 1)

IV. CONCLUSIONS

A relatively simple calculational technique has been devised to solve the integral equation that relates the experimentally measured cross section to the true cross section. This technique is relatively free of the problems encountered in previous methods, viz, the stability of the calculation technique and consequent sensitivity to scatter in the data. Scatter, of course, did affect the present results, but moderate amounts of scatter do not destroy the stability of the calculation. In fact, in the numerically simulated experiments, if the solution is smoothed by passing a curve through the midpoints of the linear segments constituting the solution, a nearly exact solution is obtained. This smoothing of the solution was applied in the second example described in Section III. Smoothing of the raw data generally results in a smoother solution, just as with any of the other techniques.

If the energy distribution of the beam is poorly known, this uncertainty will carry over into the solution. On the other hand, unless the beam is nearly monoenergetic compared to the width of the resonance peak of the cross section, a significant improvement in the estimation of the true cross section can be expected by applying the present deconvolution technique.

For the important and practical case of a translated Maxwellian beam energy distribution, an exact solution has been found for the case of constant-beam temperature. Since the result contains the derivative of the measured cross section, the numerical accuracy of results obtained from this solution are limited.

LABORATORY OPERATIONS

The Laboratory Operations of The Aerospace Corporation is conducting experimental and theoretical investigations necessary for the evaluation and application of scientific advances to new military concepts and systems. Versatility and flexibility have been developed to a high degree by the laboratory personnel in dealing with the many problems encountered in the nation's rapidly developing space and missile systems. Expertise in the latest scientific developments is vital to the accomplishment of tasks related to these problems. The laboratories that contribute to this research are:

Aerophysics Laboratory: Launch and reentry aerodynamics, heat transfer, reentry physics, chemical kinetics, structural mechanics, flight dynamics, atmospheric pollution, and high-power gas lasers.

Chemistry and Physics Laboratory: Atmospheric reactions and atmospheric optics, chemical reactions in polluted atmospheres, chemical reactions of excited species in rocket plumes, chemical thermodynamics, plasma and laser-induced reactions, laser chemistry, propulsion chemistry, space vacuum and radiation effects on materials, lubrication and surface phenomena, photo-sensitive materials and sensors, high precision laser ranging, and the application of physics and chemistry to problems of law enforcement and biomedicine.

Electronics Research Laboratory: Electromagnetic theory, devices, and propagation phenomena, including plasma electromagnetics; quantum electronics, lasers, and electro-optics; communication sciences, applied electronics, semiconducting, superconducting, and crystal device physics, optical and acoustical imaging; atmospheric pollution; millimeter wave and far-infrared technology.

Materials Sciences Laboratory: Development of new materials; metal matrix composites and new forms of carbon; test and evaluation of graphite and ceramics in reentry; spacecraft materials and electronic components in nuclear weapons environment; application of fracture mechanics to stress corrosion and fatigue-induced fractures in structural metals.

Space Sciences Laboratory: Atmospheric and ionospheric physics, radiation from the atmosphere, density and composition of the atmosphere, aurorae and airglow; magnetospheric physics, cosmic rays, generation and propagation of plasma waves in the magnetosphere; solar physics, studies of solar magnetic fields; space astronomy, x-ray astronomy; the effects of nuclear explosions, magnetic storms, and solar activity on the earth's atmosphere, ionosphere, and magnetosphere; the effects of optical, electromagnetic, and particulate radiations in space on space systems.

THE AEROSPACE CORPORATION
El Segundo, California